Journal of Trace Elements in Medicine and Biology 77 (2023) 127143

Contents lists available at ScienceDirect

Journal of Trace Elements in Medicine and Biology

journal homepage: www.elsevier.com/locate/jtemb

Tracking soluble and nanoparticulated titanium released *in vivo* from metal dental implant debris using (single-particle)-ICP-MS

Diogo Pompéu de Moraes [a,b,1], Sara González-Morales [a,b], Jorge Toledano-Serrabona [c,d], M. Ángeles Sánchez-Garcés [c,d], Jörg Bettmer [a,b], María Montes-Bayón [a,b,*], Mario Corte-Rodríguez [a,b,*]

[a] Department of Physical and Analytical Chemistry, Faculty of Chemistry, University of Oviedo, Julián Clavería 8, 33006 Oviedo, Spain
[b] Instituto de Investigación Sanitaria Del Principado de Asturias (ISPA), Av. Hospital Universitario s/n, 33011 Oviedo, Spain
[c] Department of Oral Surgery and Implantology, Faculty of Medicine and Health Sciences, University of Barcelona, Feixa Llarga s/n, L'Hospitalet de Llobregat, 08907 Barcelona, Spain
[d] Bellvitge Biomedical Research Institute (IDIBELL), Gran Via de l'Hospitalet 199, 08908 L'Hospitalet de Llobregat, Spain

ARTICLE INFO

Keywords:
Titanium nanoparticles
SP-ICP-MS
Enzymatic digestion
Alkaline extraction
Biological tissues

ABSTRACT

Background: This work studies the presence of the Ti, Al and V metal ions and Ti nanoparticles released from the debris produced by the implantoplasty, a surgical procedure used in the clinic, in rat organs.
Methods: The sample preparation for total Ti determination was carefully optimized using microsampling inserts to minimize the dilution during the acid attack of the lyophilized tissues by a microwave-assisted acid digestion method. An enzymatic digestion method was optimized and applied to the different tissue samples in order to extract the titanium nanoparticles for the single-particle ICP-MS analysis.
Results: A statistically significant increase was found for Ti concentrations from control to experimental groups for several of the studied tissues, being and particularly significant in the case of brain and spleen. Al and V concentrations were detected in all tissues but they were not different when comparing control and experimental animals, except for V in brain. The possible presence of Ti-containing nanoparticles mobilized from the implantoplasty debris was tested using enzymatic digestions and SP-ICP-MS. The presence of Ti-containing nanoparticles was observed in all the analyzed tissues, however, differences on the Ti mass per particle were found between the blanks and the digested tissue and between control and experimental animals in some organs.
Conclusion: The developed methodologies, both for ionic and nanoparticulated metal contents in rat organs, have shown the possible increase in the levels of Ti both as ions and nanoparticles in rats subjected to implantoplasty.

1. Introduction

The use of Ti-based alloys for dental implants has increased dramatically with the age of the population. According to recent published data, about 6% of the world population was carrying dental implants in the year 2016 [1]. Metal implants made of Ti-Al-V alloys show elevated rates of success but failures might come from peri-implant biological complications [2,3]. These range from reversible inflammatory lesions that affect the soft tissues surrounding a dental implant in the absence of radiographic bone loss, to the pathological condition affecting the hard and soft tissues around an osseointegrated dental implant (known as peri-implantitis) [4]. Once this pathological condition occurs, different treatment modalities have been proposed and tested in the literature, but no standard treatment protocol has been

Abbreviations: SP-ICP-MS, Single-particle Inductively Coupled Plasma Mass Spectrometry; ICP-MS, Inductively Coupled Plasma Mass Spectrometry; NPs, Nanoparticles; ICP-TQ-MS, Triple Quadrupole-Inductively Coupled Plasma Mass Spectrometer; MW-AD, Microwave-assisted Acid Digestion; SDS, Sodium Dodecyl Sulfate; TEM, Transmission Electron Microscopy; RSD, Relative Standard Deviation; LOD, Limit of Detection; LOQ, Limit of Quantification; TiNPs, Titanium-containing Nanoparticles.

* Corresponding authors at: Department of Physical and Analytical Chemistry, Faculty of Chemistry, University of Oviedo, Julián Clavería 8, 33006 Oviedo, Spain.
E-mail addresses: montesmaria@uniovi.es (M. Montes-Bayón), cortemario@uniovi.es (M. Corte-Rodríguez).
[1] Present and permanent address of the first author (D.P.M.): Institute of Chemistry, Universidade Federal do Rio Grande do Sul, 91501-970, Porto Alegre, RS, Brazil.

https://doi.org/10.1016/j.jtemb.2023.127143
Received 24 October 2022; Received in revised form 26 January 2023; Accepted 21 February 2023
Available online 23 February 2023

proven superior or completely effective [5,6]. Surgical interventions have demonstrated that are more favorable outcomes in cases of peri-implantitis [6]. Among these, evidence supports the application of resective, reconstructive, or combined approaches to limit progressive bone loss and achieve soft tissue health. In this regard, implantoplasty has been proposed as a mechanical method to smooth the dental threads while detoxifying the implant surface reducing bacterial adhesion and facilitating hygiene by the patient [7]. However, this treatment generates the production of micro- and nano-metallic debris in the peri-implant environment that can be the cause of further complications [8,9].

The measurement of metallic debris from metal implants has been accomplished previously in our group using *in vitro* approaches in the presence of artificial saliva and buccal bacteria [10]. Using single particle-inductively coupled plasma-mass spectrometry (SP-ICP-MS), it was possible to describe the occurrence of nanoparticles containing Ti, V and Al from the implants and to evaluate the evolution of these species upon formation of a bacterial biofilm on the surface of the dental implant. All these *in vitro* approximations are adequate to study metal release from a chemical point of view. However, the complete buccal biological environment and the motion of the implants are not considered.

The importance of the determination of these metal sub-products remains in their potential toxicity to human beings. In fact, titanium dioxide has been classified as a Group 2B carcinogen ("possibly carcinogen to humans") by the International Agency for Research on Cancer [11], and its use in food products as the ingredient E171 has been already banned in the European Union [12]. In the same direction, the other elements commonly present in implant alloys, such as Al and V, are known to be neurotoxic [13] and show different concentration levels in gastrointestinal, urinary and reproductive system [14]. Therefore, the release and interaction with these metals is beginning to represent a public health concern.

In the present work, an *in vivo* study using animal (rat) models has been conducted to address the mobilization of metal ions and particles from implantoplasty debris [15]. Practically, rats having a mandibular bone defect were filled with metallic debris released during implantoplasty and metal/nanoparticle translocation of Ti, V and Al was evaluated in lungs, brain, liver and spleen after animal euthanasia one month later. Since the expected metal release is very low, tissue samples were freeze-dried before analysis and further acid-digested for total elemental analysis using triple quadrupole ICP-MS. Careful optimization of the digestion conditions using microsampling inserts, as well as the application of different combination of acids, have been conducted to achieve quantitative total metal recoveries in the tissues [16]. But oral exposure to implantoplasty debris by swallowing of (nano)particles might also contribute to the total oral exposure of metals. Information on the extent of oral absorption of these particles would provide evidence on whether internal exposure is possible and on their potential to accumulate in specific tissues. However, the sample preparation to extract intact nanoparticles from biological tissues is probably one of the most challenging research areas in this context [17,18].

Most studies for solubilization of the tissues use tetramethylammonium hydroxide (TMAH) or enzymatic treatments (*e.g.* proteinase K) that have provided successful results, for instance, in the case of gold nanoparticles (NPs) [19]. However, quantitative data revealed significant lower recovery of the sought species after enzymatic digestion due to inferior transport efficiency of these nanoparticles in the presence of enzymatically digested tissue residues [18]. In addition, a main limiting factor in the case of the analysis of TiO_2 nanoparticles is their ubiquitous character in the buffers or enzymatic preparations that hamper their determination at low concentration levels in challenging biological samples. Thus, the present work illustrates the study of different digestion conditions for total and nanoparticulated Ti, Al and V in tissues from rats exposed to metal debris from implantoplasty with emphasis in the contribution of the blanks.

2. Experimental

2.1. Instrumentation

All measurements were performed with a triple quadrupole ICP-TQ-MS (iCAP, Thermo Fischer Scientific, Bremen, Germany) equipped with a Micro Mist nebulizer and a cyclonic spray chamber (both obtained from ESI Elemental Service & Instruments GmbH, Mainz, Germany). The sample introduction system was associated with an autosampler ASX-560 (Teledyne CETAC Technologies, Omah, NE, USA). The instrument was optimized daily according to manufacturer recommendations to achieve the highest sensitivity using a tuning solution. The single particle ICP-MS (SP-ICP-MS) measurements were performed using a dwell time of 5 ms and acquisition time for each run of 120 s. Transport efficiency and flow rate were daily measured. Typical operating conditions of the ICP-TQ-MS are shown in Table 1.

A microwave oven (Ethos-1, Milestone, Sorisole, Italy) equipped with 5 TFM standard vessels (SK-10 T and rotor type HPR-1000/10 S) with an internal volume of 100 mL (operating pressure and temperature up to 100 bar and 260 ºC, respectively) was used to contain 3 position rack inserts. The microsampling TFM vials (PN 33607, Milestone) were used for the digestion of lyophilized samples for subsequent determination of total concentration of Al, Ti, and V by ICP-MS. The temperature was monitored in real time during sample digestion in the reference vessel using a probe.

Other instrumentation was also used, such as a freeze dryer (Heto Lyolab 3000, Thermo Fisher Scientific, Hamburg, Germany), centrifuges (Biofuge Stratos, Thermo Fisher Scientific and MiniSpin Plus, Eppendorf, Hamburg, Germany), vortex (Reax Top, Heidolph Instruments, Schwabach, Germany), pH-meter (SensION+ PH3, Hach, Barcelona, Spain), thermoblock (ThermoMixer C, Eppendorf, Hamburgo, Germany), and ultrasonic bath (Ultrasons 30000514, J.P. Selecta, Barcelona, Spain). An analytical balance (MSD205DU/M, Mettler Toledo) with an accuracy of 0.0001 g was used to prepare all the samples, analytical standards and to perform all dilutions.

2.2. Reagents and solutions

Ultrapure water obtained in a Purelab flex 3 system (ELGA VEOLIA, Lone End, United Kingdom) with a minimum resistivity of 18.2 MΩ cm at 25 ºC was used to prepare all the standards solutions, reagents and to perform dilutions prior to analysis. Concentrated nitric acid 65% (m/m) (Acros Organics, Thermo Fisher Scientific), distilled in a sub-boiling system (DTS-1000 Acid Purification System, Savillex, Eden Prairie, USA), and concentrated hydrofluoric acid 40% (m/m) (Alfa Aesar, Thermo Fisher Scientific. 99.99% metal basis) were used for sample digestion. The purification of concentrated nitric acid by sub-boiling

Table 1
ICP-TQ-MS instrumental parameters for total Al, Ti, and V determination and operating conditions of single particle-ICP-MS for nanoparticles characterization.

Parameter	
RF Power, W	1550
Coolant gas flow, L min^{-1}	14.0
Auxiliary gas flow, L min^{-1}	0.8
Nebulizer gas flow, L min^{-1}	1.0286
CR Lens, V	-148
Extraction Lens 2, V	-180
Q1 masses, *m/z*	27 ($^{27}Al^+$), 45 ($^{45}Sc^+$), 47 ($^{47}Ti^+$) and 51 ($^{51}V^+$) Open in SQ-mode
Q3 masses, *m/z*	27 ($^{27}Al^+$), 45 ($^{45}Sc^+$), 63 ($^{47}Ti^{16}O^+$) and 67 ($^{51}V^{16}O^+$)
Single-particle ICP-MS	
Dwell time, ms	5
Sample flow rate, mL min^{-1}	0.44 – 0.47
Run time, s	120

distillation was conducted in the LO setting (lowest distillation rate) and an initial cleaning protocol to produce trace metal grade acid was performed using a double distillation of ultrapure water.

For total Al, Ti, and V quantification by ICP-MS in the samples obtained after microwave-assisted digestion, standard solutions were prepared daily by sequential dilution of a single-element stock solution containing 1000 mg L^{-1} of Al (High Purity Standards, Charleston, USA), Ti (CertiPUR, ICP Standard, Merck, Germany), and V (CertiPUR, ICP Standard, Merck, Germany) in 2% (v/v) HNO_3/HF. The range was between 0 and 5 μg L^{-1} with a final concentration of HF in the calibration standards as low as 25 μg mL^{-1} to preserve the HF-sensitive parts of the instrument. An internal standard of Sc at final concentration of 2 μg L^{-1} was added to blanks, standards, and diluted samples.

The calibration of SP-ICP-MS for the quantification of Ti-based nanoparticles was performed using Ti standard solutions prepared in ultrapure water in the range of 0–50 μg L^{-1}. These standard solutions were prepared using an intermediate single-element solution of 1000 μg L^{-1} prepared in 2% (v/v) HNO_3/1% (v/v) HF for Ti.

For optimization and spiking experiments, a commercial TiO_2 nanopowder (<25 nm, anatase, 99.7% trace metals basis) was used (Sigma-Aldrich, Madrid, Spain).

Argon (99.999%) and oxygen (99.995%), both from Air Liquide (Valladolid, Spain) were used for ICP-MS operation and for the reaction cell, respectively.

All laboratory materials such as glassware, polypropylene vials and other flasks were cleaned before use by soaking in 5% (v/v) HNO_3 bath for seven days followed by rinsing with ultrapure water.

2.3. Samples and in vivo study protocol

The *in vivo* experiments were conducted at the University of Barcelona upon approval by the Ethical Committee for Animal Experimentation of the University of Barcelona (protocol identification number 10799). In summary, a randomized experimental study was carried out in 18 Sprague-Dawley rats, with a 50% sex ratio at the population level, 6–8 months of age and with weights between 380 and 450 g. All animals were randomly distributed into two study groups: experimental group (ten rats with a unilateral mandibular defect filled with metal debris) and control group (eight rats with an empty unilateral mandibular defect). Metal particles used to fill the mandibular defect were obtained by a simulated implantoplasty procedure on Ti-6Al-4 V dental implants (Avinent Implant System S.L., Santpedor, Spain). More details about the surgical protocol and the biological implications of the *in vivo* study were described in a previous publication [20].

The samples evaluated in this study for metal ions distribution (Al, Ti, and V total concentration) and nanoparticulated Ti in the different organs were taken 30 days after surgery. The liver, spleen, brain, and lungs were extracted and frozen at − 80 °C for subsequent lyophilization. The blood samples were collected from the population of study before and after surgical procedure, frozen at − 80 °C and lyophilized. All samples were ground manually in an agate mortar and stored in polypropylene vessels at − 18 °C until use for the microwave-assisted acid digestion or enzymatic digestion.

2.4. Microwave-assisted acid digestion using microsampling inserts (MW-AD)

Two microwave-assisted acid digestion methods were used. First trials were conducted in 100 mL Teflon vessels using 0.1 g of dry tissue and adapting a digestion protocol without the use of HF, as suggested in the literature [17]. A second method was then used in order to minimize the dilution of the samples, which included the use of microsampling inserts in the digestion vessels and a different acid mixture. In this case, 0.1 g of dried and milled samples were digested using a mixture of 25 μL of HF and 2 mL of HNO_3 in TFM microsampling inserts. For the use of microsampling inserts in the conventional MW system, the 100 mL microwave vessels were loaded with 10 mL of ultrapure water and a rack with three inserts was fixed inside of the vessels. The vessels were closed and fixed on the rotor and a temperature probe (thermocouple, ATC-400-CE) was installed in the reference vessel for internal temperature monitoring and control. The optimized heating program is shown in the Table 2.

The digested solution was collected in polypropylene flasks and filled up to 25 mL with ultrapure water. Before the quantitative determination, the digested samples and analytical blanks were diluted 10 times to reduce the concentration of HF (below 100 μg mL^{-1}) to avoid damages to the quartz torch and glass sample introduction system of the ICP-MS instrument.

A cleaning step of the TFM microsampling inserts was performed using 2 mL of 50% (v/v) HNO_3 and 25 μL of concentrated HF.

2.5. Enzymatic digestion for the extraction of Ti nanoparticles

For the enzymatic extraction, the optimum conditions were achieved with the use of proteinase K as extraction enzyme to reach a complete solubilization of liver tissues based on the works of Loeschner [18] and Soto-Alvaredo [21]. In this way, 25 mg of dried and milled tissue samples were suspended in 1.5 mL of freshly prepared enzymatic solution (3 mg mL^{-1} of proteinase K, 0.5% SDS, 10 mmol L^{-1} TRIS buffer, pH 7.4–8.2). The suspension was sonicated for 1 h and finally shaken overnight at 37 °C. The enzymatic digestion solution was filled up with ultrapure water to a final volume of 2 mL. The final solution was immediately analyzed or stored at 4 °C, if necessary. Prior to analysis by SP-ICP-MS, the digested solution was sonicated for 5 min and diluted 10 times in ultrapure water.

2.6. Single-particle ICP-MS measurement of the digested tissues

The enzymatically digested tissues were measured by SP-ICP-MS using the triple-quadrupole iCAP TQ ICP-MS system with the standard sample introduction system formed by a cyclonic spray chamber and a MicroMist nebulizer of 0.4 mL min^{-1} optimal flow. For this aim, the dwell time was reduced to 5 ms with an acquisition time of 120 s per run. The Ti was monitored *via* the isotope ^{47}Ti to avoid the interference of ^{48}Ca on the most abundant ^{48}Ti. The Ti was measured in the mass shift, using O_2 as a reaction gas in the reaction cell to transform the $^{47}Ti^+$ selected in the first quadrupole into $^{47}Ti^{16}O^+$ that is detected after selecting m/z 63 in the third quadrupole with no significant interferences.

The transport efficiency was determined daily by the particle number method[22] using 30 nm standard gold nanoparticles (LGCQC5050, LGC Standards, United Kingdom) after appropriate dilution down to a concentration of $3{\cdot}10^4$ particles per mL. Under these conditions, the transport efficiency ranged from 2.5% to 3.5%. All data were exported as text files and further processed using Microsoft Excel 365. The operational parameters for the ICP-MS measurements are summarized in Table 1.

2.7. TEM measurements

Transmission electron microscopy (TEM) images were obtained with a MET-JEOL-JEM-1011 (Tokyo, Japan) operated at 100 kV. TiO_2

Table 2
Optimized conditions of the microwave-assisted acid digestion (MW-AD).

Step	Time, min	Temperature, °C	MW Power, W
1	15	Room temperature up to 90	1000
2	15	90 – 140	1000
3	15	140 – 200	1000
4	10	200	1000
5	60	Cool down to room temperature	0

standard nanoparticles suspensions at a concentration of 1 mg mL^{-1} and the enzymatically treated liver tissue were sonicated for 5 min prior to TEM imaging.

3. Results

3.1. Optimization of the microwave-assisted acid digestion (MW-AD) method

As a starting point to attempt the digestion of the freeze-dried tissues, previously published strategies[18,21] were used with some modifications that will be detailed in the following section. The optimization of the MW-AD method was performed using Ti as the target element of interest. The best conditions obtained for Ti were then applied for Al and V.

3.2. Evaluation of the effect of the acid mixture on the recovery of ionic Ti and Ti nanoparticles

The first digestion experiments (without addition of HF) and following the work of Loeschner[18] and Soto-Alvaredo[21] provided recoveries of Ti only up to 60%. Spiking experiments with TiO_2 nanoparticles resulted in even lower recoveries about 15% with poor precisions, higher than 30%.

To improve the recoveries, HF was further used in the acid mixture. The addition of only 25 μL of concentrated HF increased the recovery of soluble Ti to (96.5 ± 7.3) %, with RSDs below 5%. However, the recovery of spiked TiO_2 nanoparticles was still below 25% and high analytical blanks and cross-contamination between samples was observed.

At least 0.5 mL of HF were needed to obtain quantitative recoveries (> 95%) for spiked TiO_2 NPs (5 and 10 mg). Such high volumes imply the need to apply high dilution factors up to 250-fold to avoid any damage to the glassware and quartz of the sample introduction system. Therefore, since the contribution of TiO_2 nanoparticles to the total Ti determination in these biological samples was expected to be minimal (more details are discussed in the section of SP-ICP-MS analysis), only 25 μL of HF were added to the digestion mixture.

3.3. Optimization of microwave digestions using TFM microsampling inserts

The use of microsampling inserts allows to reduce the mass of sample and the digestion volume, which are limited to 0.1 g and 3 mL, respectively. An initial experiment was conducted using 0.1 g of dry tissue and a solution of 1 mL of H_2O, 1 mL of HNO_3, 0.5 mL H_2O_2, and 25 μL of HF. The microwave heating program was the same as described in Table 2. A significant reduction of the blanks for all analytes was observed when comparing to the blanks obtained using TFM vessels of 100 mL. However, a low repeatability, with RSDs up to 30% (N = 3), was obtained for the samples spiked with soluble Ti.

In order to avoid sample projections that could be caused by a gas overpressure in the digestion inserts, a second experiment was carried out by eliminating the H_2O_2 and using 2 mL of HNO_3 together with 25 μL of HF as acid digestion mixture. As a result, lower standard deviation and analytical blanks were obtained, resulting in LODs of 0.370, 0.022, 0.004 μg L^{-1} (calculated as 3 times the standard deviation of blanks divided by the slope of the calibration curve)[2] for Al, Ti, and V, respectively, that turned to 39, 1.75 and 0.51 ng g^{-1} referring to the dried tissue when taking into account the dilution factors applied to the original sample during the digestion and measurement. The use of microsampling inserts also increased the sample throughput, since up to three inserts can be set in one digestion vessel.

When applying these digestion conditions, the concentrations of Al, Ti and V could be quantified in the different organs and blood and the results were carefully discussed in a previous publication.[20].

In summary, Fig. 1 shows these results. The concentration of Ti in all analyzed organs ($p < 0.05$, Fig. 1c) and V in brain samples ($p = 0.016$, Fig. 1b) showed a statistically significant increase in the experimental group. Moreover, the results on blood samples of the animals, collected before and after the surgery are shown in Fig. 2. In this case, although no statistically significant differences were observed between control and experimental groups, there is an evident trend to higher Ti levels after the surgery, both in control and experimental groups. The only significant difference ($p < 0.05$) was found in Al between control and experimental animals. Surprisingly, in this case the Al content was lower in

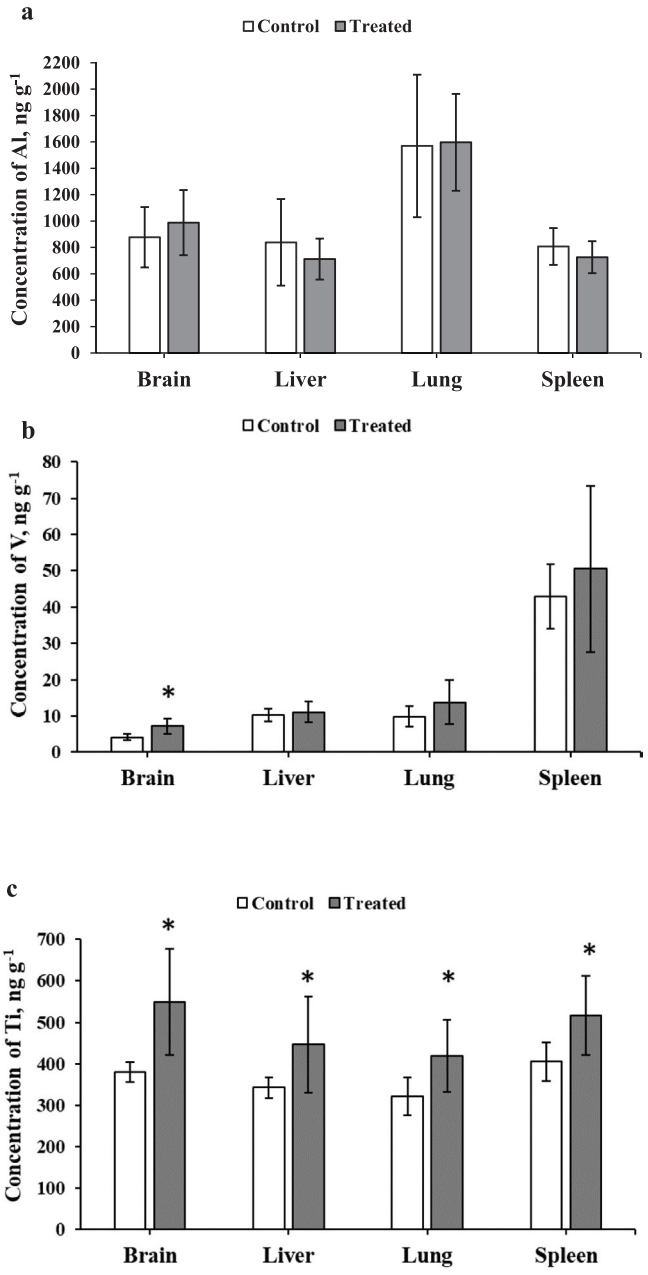

Fig. 1. Results obtained for total concentration of (a) Al, (b) V, and (c)Ti by ICP-TQ-MS after MW-AD in the biological samples of proposed study. The bars represent the average of control (white) and treated (gray) groups. Error bars are the standard deviation. Asterisks show significant differences ($p < 0.05$) between the experimental and the corresponding control groups.

[2] The values for LOQs were 1.23, 0.073 and 0.013 μg L^{-1} for Al, Ti and V, respectively.

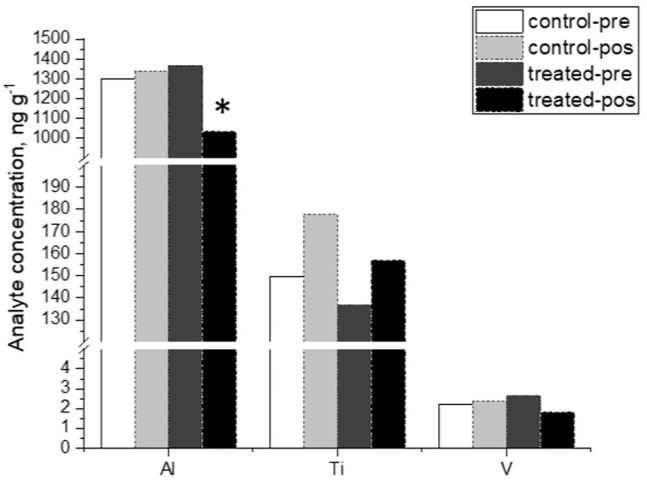

Fig. 2. Results for total concentration of Al, Ti, and V in blood samples by ICP-MS after MW-AD. The bars represent the average for control (white) and treated (gray) groups before and after surgical procedure. Error bars are the standard deviation. Asterisks show significant differences ($p < 0.05$) between the experimental and the corresponding control groups.

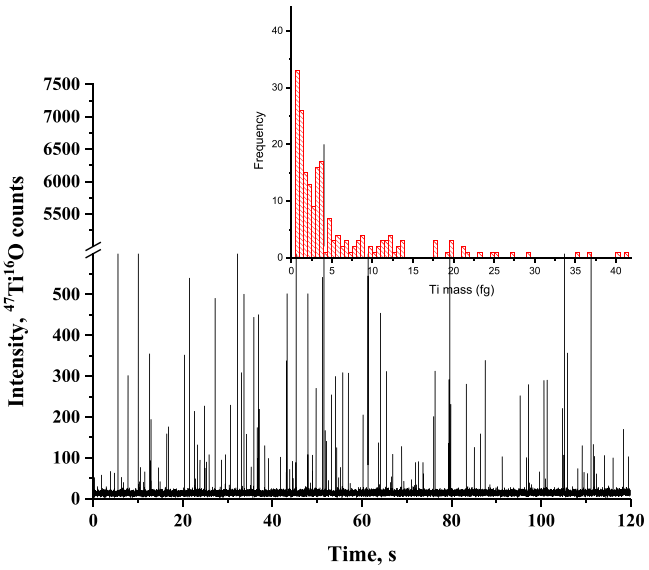

Fig. 3. Enzymatically digested liver sample spiked with TiO_2 nanoparticles. The insets show the mass distribution histograms for each sample.

the animals that were subjected to the surgery than in the controls. This might be ascribed to natural differences in the basal levels of this metal, rather than to the surgical procedure itself.

3.4. Extraction of Ti nanoparticles from rat tissues and analysis by SP-ICP-MS

For extraction of the existing nanoparticles in the tissues, firstly, a combination of lipase and pancreatine was used following previous publications.[17,23] This led to a cloudy suspension that had to be filtered and/or centrifuged prior to SP-ICP-MS analysis, causing an important loss of nanoparticles. Secondly, a modified protocol[18,21] using a combination of proteinase K and SDS in Tris buffer succeeded to hydrolyze peptide bonds and solubilize fatty acids and other low-solubility components of the tissue. This treatment resulted in a homogeneous solution free of solid matter. In Fig. S1, a visual comparison of the suspensions obtained by both enzymatic digestion methods can be seen.

The overall analytical recovery of the extraction method was evaluated by spiking a liver sample (before extraction) with a standard of TiO_2 nanoparticles at a concentration of 80 μg kg^{-1} of Ti before dilution with ultrapure water. The raw signals and their corresponding mass histogram are shown in Fig. 3. As can be seen, the number of events is significantly higher than in the blank (1362 events *versus* 160), while the background signal is not really affected.

Taking into account the mass of TiO_2 nanoparticle standard added to this sample, and the number of particles detected in the final dilution, the recovery for the spiked liver sample of Fig. 3 turned out to be about 30%, which agrees with the non-quantitative recoveries observed by other authors.[18] It must be taken into account, however, the complexity of this determination, since the nanoparticle standard is added to the freeze-dried samples, which are then subjected to an enzymatic digestion. Thus, a significant loss of nanoparticles in the samples by precipitation, adsorption or solubilization processes is expectable.

Since a relatively high presence of TiNPs was found in the blank solutions, including ultrapure water and digestion blanks, it was important to minimize their contribution to the analysis, particularly in the case of samples where the concentrations are extremely low. In this regard, it was necessary to conduct a thorough washing of polypropylene bottles in 10% HNO_3 overnight, discarding, at least, 1 L of ultrapure water before actually collecting the amount needed for the day, and filtering buffers using 3 kDa cutoff filters to have a significant decrease on the obtained blanks. However, some reagents, like the enzymes used for digestion buffers, were not suitable to any cleaning procedure and had an impact on the background signals. After taking these precautions, the blank solution contained only around 20 titanium events in a typical 120 s run (data not shown). However, the digestion blank, containing the proteinase K, SDS and Tris buffer, contained a significant number of Ti events (146).

A digested liver sample is shown, as an example, in Fig. 3. As can be seen, the number of events (199 events) is not significantly different to this in the digestion blank (146 events).

After appropriate calculations shown in previous publications[10], event intensities were transformed into mass of Ti per event by means of an external calibration using ionic elemental Ti standards. The detection limit of TiO_2 NPs under these experimental conditions turned out to be 2.1 fg of TiO_2 or 1.3 fg of Ti per particle. After obtaining the mass of Ti in each event, the data sets were plotted as box and whiskers plots

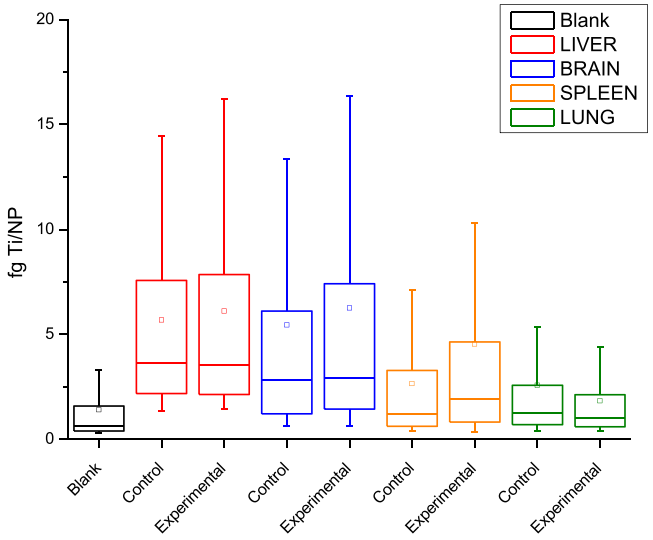

Fig. 4. Boxplot graph that shows the mass distribution of the particles found in the digestion blank and samples of liver, brain, spleen and lung. For each organ, the first box corresponds to a control rat, and the second box corresponds to an experimental rat.

(boxplots) that are shown in Fig. 4. Each box is constructed as a merge of two independent digestions of the same sample (blank, treated or control), which were not statistically different before being merged. Fig. 4 shows a comparison of the Ti mass in a digestion blank and the results obtained for each organ, comparing a control rat (control) with an implanted rat (experimental). The obtained statistical descriptors are also summarized in Table 3.

4. Discussion and conclusions

The effect of metal/nanoparticles translocation *in vivo* using rat models and using just a short exposure period (30 days) has been tackled in this work. The limited amount of sample, together with the low expected concentrations of the analytes in the tissues were the main analytical challenges that needed to be faced in the total elemental analysis section. Out of the two mentioned digestion methods, the use of relatively high HF amounts was required for quantitative recoveries of nanoparticulated titanium, which was not compatible with the glass and quartz sample introduction system as suggested by previous studies.[25,26]. Therefore, a compromise solution was chosen with a minimal amount of HF, assuming that the concentration of nanoparticulated Ti would be, in any case, low. It is also worth mentioning that, in addition to Ti, the use of HF was also recommended by Loeschner et al.[27] to achieve a complete dissolution of aluminum compounds present in particulate form, such as aluminum silicate.

As a drawback, when using HF, a significant increase in the analytical blanks and cross contamination between different samples was observed, as previously described by Zhang et al. [28].

To solve the problems related with blanks and limited sample amount, the microsampling inserts allowed to reduce the sample and reagents amounts needed for reliable results on the analysis of Ti and the other elements in the samples even at ultra-trace concentration [29]. In addition, the removal of H_2O_2 in the digestion mixture, whose oxidizing action was undertaken by concentrated HNO_3[30], also helped to obtain a better reproducibility, which, in combination with an optimized digestion program with slow temperature ramps allowed acceptable precisions, according to the complexity of the analyzed material.

Such conditions permitted to achieve low detection limits allowing the determination of the elements of interest in the samples. Most significant differences were found in the content of Ti, where the increased concentrations in the experimental group of animals indicated that a change in the distribution of this element might have been induced by the implantoplasty with subsequent translocation of metallic particles and/or Ti ions [20]. It is not surprising that Ti is the only metal showing significant differences between control and experimental groups. This is probably due to the composition of the dental implants, being an alloy of Ti (base metal) with 6% of Al and 4% V. Therefore, Al and V are minor components of this material, and their biological concentrations are consequently much lower. In fact, only V in brain was slightly significantly increased in the treated rat group.

When it comes to the concentration of Al in all tissues, it was in the order of 1000 ng g^{-1} and in agreement with basal levels of Al in rat tissues previously reported [31]. The average concentration of V was around 10 ng g^{-1} for brain, liver and lung tissues. However, the V concentration in the spleen was around 5 times higher. As described for Al, the V concentrations obtained in this work are in line with previous values reported for V in rat tissues [32,33].

As previously shown, the metallic debris obtained after implantoplasty (using titanium as representative element of this process) may be composed by low-molecular weight species or ions, but also, nanoparticles. To investigate the production and translocation of Ti-containing nanoparticles (TiNPs) by the implantoplasty procedure, single particle ICP-MS (SP-ICP-MS) seems the ideal tool once the tissues are specifically processed using enzymatic solubilization in the presence of SDS.

As shown in the results section, one main concern is the presence of TiNPs in blank solutions that can not be eliminated by filtration and/or centrifugation procedures. However, the calculations revealed that the particles contributing to the blanks have a mass of about 5 fg of Ti, or even lower, which is very close to the detection limit. When analyzing the number of particles found after the digestion of the liver, roughly the same number of particles were detected in both the blank sample and the digested liver, probably suggesting that the presence of TiNPs in this tissue, if any, is very low. In addition, the increase in the continuous background confirmed the presence of Ti in other forms than NPs in the samples already observed in the total Ti determination [34].

It is noteworthy that in all analyzed organs, the mass of Ti in the TiNPs found in both, control and experimental groups, corresponded to much larger particle sizes than those present in the digestion blanks, but very similar between control and experimental groups (considering spherical and pure TiO_2 nanoparticles). This finding supports the idea that the rats incorporated omnipresent titanium through feeding, water, and contact with materials. These results, however, reveal that the nanoparticles produced and transported from the implanted area to most of the analyzed organs were either very few or too small to be detected with the used strategy (the animals were exposed for only one month).

For the case of brain and spleen, however, the interpretation is slightly different. The particles found in controls are not statistically different from those found in experimental samples. However, there is a clear increase in the higher-mass particles in the experimental rats revealed by the growth in the third quartile in Table 3. This demonstrates a small difference in the organs from the experimental animals that contain, at least, a population of bigger-sized particles than those present in the control animals. This may indicate either a production of bigger TiNPs due to increased Ti levels (as demonstrated already in the total ionic titanium quantification) or an accumulation of bigger particles that are transported from the implant site. The possible presence of larger sized particles as consequence of the aggregation of smaller particles should not be discarded either. This would explain that even when the number of events is not significantly higher in the samples than in the digestion blank, the obtained masses of Ti per particle, were higher in the animal tissues and among them, in the exposed animals. In fact, the preliminary TEM measurements of the extracts revealed the

Table 3
Statistical descriptors of the mass distributions of the events found in the liver, brain, spleen and lung samples. Q1 and Q3 are quartiles 1 and 3, respectively. Avg means average. SD means standard deviation of the dataset containing all events.

		Q1, fg	Q3, fg	Median, fg	Avg, fg	SD, fg	# Events
	Blank	0.39	1.60	0.65	1.40	2.00	300
Liver	**Control**	2.19	7.57	3.66	5.68	5.11	126
	Experimental	2.13	7.84	3.53	6.11	5.88	223
Brain	**Control**	1.21	6.10	2.83	5.45	7.36	682
	Experimental	1.44	7.39	2.93	6.25	8.48	391
Spleen	**Control**	0.62	3.28	1.23	2.65	3.37	380
	Experimental	0.82	4.60	1.90	4.54	7.99	619
Lung	**Control**	0.70	2.57	1.26	2.58	4.55	446
	Experimental	0.59	2.12	1.01	1.83	2.05	519

presence of small particle aggregates that might be due to the presence of TiNPs, although elemental analysis could not be done (Fig. S2).

In conclusion, the analytical challenge of evaluating metal and metal nanoparticles translocation in the organs of implanted rats has been undertaken using exhaustive sample preparation protocols. For total elemental concentration, an optimized procedure using concentrated HF directly added on the sample and using microsampling inserts to minimize sample dilution permitted to achieve necessary LODs to accomplish the determination of Ti, Al and V in tissue samples. The only significant differences when comparing exposed and control samples could be observed in the case of Ti, and thus, the possible presence of Ti as nanoparticles was further investigated. In this regard, the use of proteinase K and SDS allowed the solubilization of the tissues. The coexistence of Ti in the form of nanoparticles and ions was proven through SP-ICP-MS experiments. Although the significant content of nanoparticulated Ti in control rats from environmental sources hampered the correct determination of the nanoparticles with an origin in the implanted debris, the mass of Ti in the obtained events seemed to point out the presence of different Ti nanoparticles in brain and spleen samples distinguishable from those in the control counterparts.

Declaration of Competing Interest

The authors declare that they have no known competing financial interests or personal relationships that could have appeared to influence the work reported in this paper.

Acknowledgements

The authors gratefully acknowledge the financial support from the Spanish MICINN (Spanish Ministry for Science, Innovation and Universities, Grant Numbers MCI-20-PID2019-104334RB-100 and RTI2018-094605-B-I00) and from FICYT (Grant number: SV-PA-21-AYUD/2021/51399). Moreover, Thermo Fisher Scientific, Bremen, Germany, is kindly acknowledged for the instrumental support (iCAP™ TQ ICP-MS). The author (Moraes, D. P.) kindly acknowledges the Coordenação de Aperfeiçoamento de Pessoal de Nível Superior – Brasil (CAPES) – Finance Code 001 for scholarship. M. Corte-Rodríguez also thanks “Instituto de Salud Carlos III” for the postdoctoral Sara Borrell contract (CD19/00249).

CRediT authorship contribution statement

Diogo Pompéu de Moraes: Investigation, Methodology, Visualization, Formal analysis, Writing – original draft. **Sara González-Morales**: Investigation, Writing – review & editing. **Jorge Toledano-Serrabona**: Conceptualization, Writing – review & editing, Resources. **M. Ángeles Sánchez-Garcés**: Conceptualization, Writing – review & editing, Resources. **Jörg Bettmer**: Writing – Review & Editing, Conceptualization. **María Montes-Bayón**: Conceptualization, Methodology, Writing – review & editing, Supervision. **Mario Corte-Rodríguez**: Conceptualization, Methodology, Writing – original draft, Investigation, Supervision.

Appendix A. Supporting information

Supplementary data associated with this article can be found in the online version at doi:10.1016/j.jtemb.2023.127143.

References

[1] W. Becker, P. Hujoel, B.E. Becker, P. Wohrle, Dental implants in an aged population: evaluation of periodontal health, bone loss, implant survival, and quality of life, Clin. Implant Dent. Relat. Res. 18 (2016) 473–479, https://doi.org/10.1111/cid.12340.

[2] T. Berglundh, G. Armitage, M.G. Araujo, G. Avila-Ortiz, J. Blanco, P.M. Camargo, S. Chen, D. Cochran, J. Derks, E. Figuero, C.H.F. Hämmerle, L.J.A. Heitz-Mayfield, G. Huynh-Ba, V. Iacono, K.T. Koo, F. Lambert, L. McCauley, M. Quirynen, S. Renvert, G.E. Salvi, F. Schwarz, D. Tarnow, C. Tomasi, H.L. Wang, N. Zitzmann, Peri-implant diseases and conditions: Consensus report of workgroup 4 of the 2017 World Workshop on the Classification of Periodontal and Peri-Implant Diseases and Conditions, J. Periodo 89 (2018) S313–S318, https://doi.org/10.1002/JPER.17-0739.

[3] L. Francetti, N. Cavalli, S. Taschieri, S. Corbella, Ten years follow-up retrospective study on implant survival rates and prevalence of peri-implantitis in implant-supported full-arch rehabilitations, Clin. Oral. Implant. Res. 30 (2019) 252–260, https://doi.org/10.1111/clr.13411.

[4] F. Schwarz, J. Derks, A. Monje, H.L. Wang, Peri-implantitis, J. Periodo 89 (2018) S267–S290, https://doi.org/10.1002/JPER.16-0350.

[5] F. Suarez, A. Monje, P. Galindo-Moreno, H.L. Wang, Implant surface detoxification: a comprehensive review, Implant. Dent. 22 (2013) 465–473, https://doi.org/10.1097/ID.0b013e3182a2b8f4.

[6] E. Figuero, F. Graziani, I. Sanz, D. Herrera, M. Sanz, Management of peri-implant mucositis and peri-implantitis, Periodontol 2000 (66) (2014) 255–273.

[7] A. Monje, R. Pons, E. Amerio, H.L. Wang, J. Nart, Resolution of peri-implantitis by means of implantoplasty as adjunct to surgical therapy: a retrospective study, J. Periodo (2021) 1–13, https://doi.org/10.1002/JPER.21-0103.

[8] F.N. Barrak, S. Li, A.M. Muntane, J.R. Jones, Particle release from implantoplasty of dental implants and impact on cells, Int. J. Oral. Max. Impl. 6 (2020) 1–9, https://doi.org/10.1186/s40729-020-00247-1.

[9] J. Toledano-Serrabona, F.J. Gil, O. Camps-Font, E. Valmaseda-Castellón, C. Gay-Escoda, M.Á. Sánchez-Garcés, Physicochemical and biological characterization of Ti6Al4V particles obtained by implantoplasty: an in vitro study. Part I, Materials 14 (2021) 6507, https://doi.org/10.3390/ma14216507.

[10] M. Cosmi, N. Gonzalez-Quiñonez, P. Tejerina Díaz, Á. Manteca, E. Blanco-González, J. Bettmer, M. Montes-Bayón, M. Corte-Rodriguez, Evaluation of nanodebris produced by in vitro degradation of titanium-based dental implants in the presence of bacteria using single particle and single cell inductively coupled plasma mass spectrometry, J. Anal. At. Spectrom. 36 (2021) 2007–2016, https://doi.org/10.1039/d1ja00154j.

[11] V.B. Antony, J.A. Bond, J.S. Brown, D. Costa, P.A. Demers, S. Hankinson, U. Heinrich, E.D. Kuempel, J.H. Olsen, R. Schins, J. Siemiatycki, H. Tsuda, M. van Tongeren, E.W. Vainio, A.G. Wylie, I.J. Yu, IARC monographs on the evaluation of carcinogenic risks to humans, 2010. https://doi.org/10.1136/jcp.48.7.691-a.

[12] Commission Regulation (EU) 2022/63, January 18, 2022, EU Official Journal.

[13] A.V. Skalny, M. Aschner, Y. Jiang, Y.G. Gluhcheva, Y. Tizabi, R. Lobinski, A. A. Tinkov, Molecular mechanisms of aluminum neurotoxicity: update on adverse effects and therapeutic strategies (in), Physiol. Behav. (2021) 1–34, https://doi.org/10.1016/bs.ant.2020.12.001.

[14] A. Wilk, D. Szypulska-Koziarska, B. Wiszniewska, The toxicity of vanadium on gastrointestinal, urinary and reproductive system, and its influence on fertility and fetuses malformations, Post. Hig. Med. Dosw. 71 (2017) 850–859, https://doi.org/10.5604/01.3001.0010.4783.

[15] M.B. Guglielmotti, M.G. Domingo, T. Steimetz, E. Ramos, M.L. Paparella, D. G. Olmedo, Migration of titanium dioxide microparticles and nanoparticles through the body and deposition in the gingiva: an experimental study in rats, Eur. J. Oral. Sci. 123 (2015) 242–248, https://doi.org/10.1111/eos.12190.

[16] I. Pujalté, D. Dieme, S. Haddad, A.M. Serventi, M. Bouchard, Toxicokinetics of titanium dioxide (TiO2) nanoparticles after inhalation in rats, Toxicol. Lett. 265 (2017) 77–85, https://doi.org/10.1016/j.toxlet.2016.11.014.

[17] M.V. Taboada-López, P. Herbello-Hermelo, R. Domínguez-González, P. Bermejo-Barrera, A. Moreda-Piñeiro, Enzymatic hydrolysis as a sample pre-treatment for titanium dioxide nanoparticles assessment in surimi (crab sticks) by single particle ICP-MS, Talanta 195 (2019) 23–32, https://doi.org/10.1016/j.talanta.2018.11.023.

[18] K. Loeschner, M.S.J. Brabrand, J.J. Sloth, E.H. Larsen, Use of alkaline or enzymatic sample pretreatment prior to characterization of gold nanoparticles in animal tissue by single-particle ICPMS characterisation of nanomaterials in biological samples, Anal. Bioanal. Chem. 406 (2014) 3845–3851, https://doi.org/10.1007/s00216-013-7431-y.

[19] R. Álvarez-Fernández García, N. Fernández-Iglesias, C. López-Chaves, C. Sánchez-González, J. Llopis, M. Montes-Bayón, J. Bettmer, Complementary techniques (spICP-MS, TEM, and HPLC-ICP-MS) reveal the degradation of 40 nm citrate-stabilized Au nanoparticles in rat liver after intraperitoneal injection, J. Trace Elem. Med. Biol. 55 (2019) 1–5, https://doi.org/10.1016/j.jtemb.2019.05.006.

[20] J. Toledano-Serrabona, O. Camps-Font, D.P. de Moraes, M. Corte-Rodríguez, M. Montes-Bayón, E. Valmaseda-Castellón, C. Gay-Escoda, M. Ángeles Sánchez-Garcés, Ion release and local effects of titanium metal particles from dental implants. An experimental study in rats, J. Periodo (2022), https://doi.org/10.1002/JPER.22-0091.

[21] J. Soto-Alvaredo, C. López-Chaves, C. Sánchez-González, M. Montes-Bayón, J. Llopis, J. Bettmer, Speciation of gold nanoparticles and low-molecular gold species in Wistar rat tissues by HPLC coupled to ICP-MS, J. Anal. At. Spectrom. 32 (2017) 193–199, https://doi.org/10.1039/c6ja00248j.

[22] H.E. Pace, N.J. Rogers, C. Jarolimek, V.A. Coleman, P. Higgins, J.F. Ranville, Determining transport efficiency for the purpose of counting and sizing nanoparticles via single particle inductively coupled plasma-mass spectrometry, Anal. Chem. 83 (2011) 9361–9369, https://doi.org/10.1021/ac201952t.

[23] M.V. Taboada-López, S. Iglesias-López, P. Herbello-Hermelo, P. Bermejo-Barrera, A. Moreda-Piñeiro, Ultrasound assisted enzymatic hydrolysis for isolating titanium dioxide nanoparticles from bivalve mollusk before sp-ICP-MS, Anal. Chim. Acta 1018 (2018) 16–25, https://doi.org/10.1016/j.aca.2018.02.075.

[25] S. Faucher, G. Lespes, Quantification of titanium from TiO2 particles in biological tissue, J. Trace Elem. Med. Biol. 32 (2015) 40–44, https://doi.org/10.1016/j.jtemb.2015.06.001.
[26] Y. Nia, S. Millour, L. Noël, P. Krystek, W. de Jong, T. Guérin, Determination of Ti from TiO2 Nanoparticles in Biological Materials by Different ICP-MS Instruments: Method Validation and Applications, J. Nanomed. Nanotechnol. 06 (2015) 1–8, https://doi.org/10.4172/2157-7439.1000269.
[27] K. Loeschner, M. Correia, C. López Chaves, I. Rokkjær, J.J. Sloth, Detection and characterisation of aluminium-containing nanoparticles in Chinese noodles by single particle ICP-MS, Food Addit. Contam. A 35 (2018) 86–93, https://doi.org/10.1080/19440049.2017.1382728.
[28] S. Zhang, X. Liang, G.M. Gadd, Q. Zhao, Advanced titanium dioxide-polytetrafluorethylene (TiO2-PTFE) nanocomposite coatings on stainless steel surfaces with antibacterial and anti-corrosion properties, Appl. Surf. Sci. 490 (2019) 231–241, https://doi.org/10.1016/j.apsusc.2019.06.070.
[29] G. Knapp, P. Schramel, Sources of analyte contamination and loss during the analytical process, in: Sample Preparation for Trace Element Analysis, Elsevier, 2003, pp. 23–45, https://doi.org/10.1016/S0166-526X(03)41002-7.
[30] E.I. Müller, M.F. Mesko, D.P. Moraes, M. das G.A. Korn, É.M.M. Flores, Wet Digestion Using Microwave Heating, in: Microwave-Assisted Sample Prep. Trace Elem. Determ., Elsevier, 2014: pp. 99–142. https://doi.org/10.1016/B978–0-444–59420-4.00004–0.
[31] A.A. Shumakova, V.A. Shipelin, N.V. Trusov, I.V. Gmoshinski, Content of essential and toxic trace elements in organs of obese Wistar and Zucker leprfa rats receiving quercetin, J. Trace Elem. Med. Biol. 64 (2021), 126687, https://doi.org/10.1016/j.jtemb.2020.126687.
[32] J. Edel, R. Pietra, E. Sabbioni, E. Marafante, A. Springer, L. Ubertalli, Disposition of vanadium in rat tissues at different age, Chemosphere 13 (1984) 87–93, https://doi.org/10.1016/0045-6535(84)90010-9.
[33] S. Treviño, A. Díaz, E. Sánchez-Lara, B.L. Sanchez-Gaytan, J.M. Perez-Aguilar, E. González-Vergara, Vanadium in biological action: chemical, pharmacological aspects, and metabolic implications in diabetes Mellitus, Biol. Trace Elem. Res. 188 (2019) 68–98, https://doi.org/10.1007/s12011-018-1540-6.
[34] A.D. Tinoco, M. Saxena, S. Sharma, N. Noinaj, Y. Delgado, E.P.Q. González, S. E. Conklin, N. Zambrana, S.A. Loza-Rosas, T.B. Parks, Unusual synergism of transferrin and citrate in the regulation of Ti(IV) speciation, transport, and toxicity, J. Am. Chem. Soc. 138 (2016) 5659–5665, https://doi.org/10.1021/jacs.6b01966.